



Article

The Effect of Land Use and Land Cover Changes on Flood Occurrence in Teunom Watershed, Aceh Jaya

Sugianto Sugianto ^{1,2,*} , Anwar Deli ^{1,3}, Edy Miswar ³, Muhammad Rusdi ^{1,2,3} and Muhammad Irham ^{3,4,5} ¹ Faculty of Agriculture, Universitas Syiah Kuala, Banda Aceh 23111, Indonesia² Remote Sensing and Cartography Lab, Faculty of Agriculture, Universitas Syiah Kuala, Banda Aceh 23111, Indonesia³ Center for Environmental and Natural Resources Research (PPLH-SDA), Universitas Syiah Kuala, Banda Aceh 23111, Indonesia⁴ Faculty of Marine and Fisheries, Universitas Syiah Kuala, Banda Aceh 23111, Indonesia⁵ Geographic Information System Laboratory of the Faculty of Maritime and Fisheries, Universitas Syiah Kuala, Banda Aceh 23111, Indonesia

* Correspondence: sugianto@unsyiah.ac.id

Abstract: The change in land use and land cover in upstream watersheds will change the features of drainage systems such that they will impact surface overflow and affect the infiltration capacity of a land surface, which is one of the factors that contributes to flooding. The key objective of this study is to identify vulnerable areas of flooding and to assess the causes of flooding using ground-based measurement, remote sensing data, and GIS-based flood risk mapping approaches for the flood hazard mapping of the Teunom watershed. The purposes of this investigation were to: (1) examine the level and characteristics of land use and land cover changes that occurred in the area between 2009 and 2019; (2) determine the impact of land use and land cover changes on the water overflow and infiltration capacity; and (3) produce flood risk maps for the Teunom sub-district. Landsat imagery of 2009, 2013, and 2019; slope maps; and field measurement soil characteristics data were utilized for this study. The results show a significant increase in the use of residential land, open land, rice fields, and wetlands (water bodies) and different infiltration rates that contribute to the variation of flood zone hazards. The Teunom watershed has a high and very high risk of ~11.98% of the total area, a moderate risk of 56.24%, and a low and very low risk of ~31.79%. The Teunom watershed generally has a high flood risk, with a total of ~68% of the area (moderate to very high risk). There was a substantial reduction in forest land, agricultural land, and shrubs from 2009 to 2019. Therefore, the segmentation of flood-risk zones is essential for preparation in the region. The study offers basic information about flood hazard areas for central governments, local governments, NGOs, and communities to intervene in preparedness, responses, and flood mitigation and recovery processes, respectively.

Keywords: infiltration capacity; land use–land cover; watershed; flood risk area; water runoff

Citation: Sugianto, S.; Deli, A.; Miswar, E.; Rusdi, M.; Irham, M. The Effect of Land Use and Land Cover Changes on Flood Occurrence in Teunom Watershed, Aceh Jaya. *Land* **2022**, *11*, 1271. <https://doi.org/10.3390/land11081271>

Academic Editors: Stefano Morelli, Veronica Pazzi and Mirko Francioni

Received: 6 July 2022

Accepted: 4 August 2022

Published: 8 August 2022

Publisher's Note: MDPI stays neutral with regard to jurisdictional claims in published maps and institutional affiliations.



Copyright: © 2022 by the authors. Licensee MDPI, Basel, Switzerland. This article is an open access article distributed under the terms and conditions of the Creative Commons Attribution (CC BY) license (<https://creativecommons.org/licenses/by/4.0/>).

1. Introduction

Frequent flood occurrence in a watershed area is not only related to upstream conditions, such as land use and land cover change (LULCC) [1,2], but also to extreme climates that lead to heavy rainfall in some areas of the Indonesia archipelago. Flood occurrence due to environmental disturbance is becoming a concern in Indonesia and globally [3–5]. The main concern about the frequent flooding is the change in land use patterns due to the increasing need for land for agriculture and other land uses. Therefore, information on the hazard risk area due to LULCC is essential for Indonesia, which has recently experienced extreme rain [6,7]. LULCC may impact flooding and riverbank damage during the rainy season and reduce the water volume during the dry season in the area. The impact can be

seen in the repetitive occurrence of flooding in Indonesia in the last decade [8], including in the Teunom watershed, Aceh Province.

The Teunom watershed and surrounding areas experienced two floods in early January of 2017 and 2016 [9], and there were four major floods, one of which was a flash flood. More floods occurred in 2016, and then two floods occurred in 2012 and 2015 [10]. Meanwhile, between 1999 and 2011, there was only one flood per year, on average, in the Teunom watershed and its surroundings [11]. There was an economic value loss of IDR ~8 billion due to the floods in 2016, where several public services did not function properly to some extent, which impacted the economy in the area [12].

The fundamental causes of repetitive flooding in this area are the result of narrowing river flows [11], sediment deposition [13], land use conversion [14], and microclimate due to land use and land cover [10]. On the other hand, according to data from the Meteorology, Climatology, and Geophysics Agency [11], there has been an increase in annual rainfall of 0.3%, particularly in the last five years. Moreover, extreme weather due to increasing sea surface temperatures and the confluence of Australian and Asian monsoons, together with land use changes, are the causes of the increased rainfall in this area [15,16]; thus, the carrying capacity of land and rivers is saturated, and water overflows cause flooding [17–19].

Floods are natural phenomena caused by natural events and human activities [20]. Floods have the potential to cause injury and environmental damage. There are several causes of flooding due to anthropogenic activities, such as the extension of residential areas, population growth, and land use and land cover change (LULCC), which impact the hydrological cycle and water availability [20]. A result of these factors, there was the increase in the level of infiltration and runoff [21,22]. Furthermore, the level of vegetation cover affects the evaporation rate, thereby changing the humidity level and affecting cloud formation [23]. Vegetation can have a significant effect on hydrological fluxes due to variations in the physical characteristics of the land surface, soil, and vegetation, such as the roughness, albedo, infiltration capacity, root depth, architectural resistance, leaf area index (LAI), and stomatal conductance [24,25]. The nature and land cover affect the runoff, infiltration, and groundwater recharge. The soil surface functions in the water cycle, where rainfall is redistributed to evaporation, runoff, and soil infiltration [26].

The increase in urbanization resulting from the conversion of forest land into agricultural land or settlements is a real change. The impact of increased deforestation on disposal processes is relatively easy to identify. In the developed area, it is indicated that an increase in the water-resistant area causes an increase in the rate of land flow [27]. This prevents the natural holding capacity of water and changes the subsoil layer or groundwater movement, leading to an increase in flood development and the volume of flood discharge [28].

The increase in the number of people and built-up patterns has caused alterations in land use–land cover [29,30] and in overseeing the necessities on land in the Krueng Teunom watershed. LULCC causes alterations in the natural drainage system [31], impacts surface runoff [31], and affects infiltration capacity [31]. These factors are believed to contribute to the frequent flooding in the Krueng Teunom watershed. Meanwhile, the level of available vegetation cover and the absorption degree also change the rate of evapotranspiration [32]. These factors change the behavior and balance that occurs between water evaporation [33], water recharge [34], and water distribution through rivers [35,36].

Vulnerability to flooding in the Krueng Teunom watershed is exacerbated by the reduction in the extension of vegetation cover [10], including forests, which are essential in stabilizing hydrological functions; collecting rainwater (overland runoff); and controlling floods [37]. According to [38], more than 40% of forests have been cleared, which opens up more space for the development of oil palm plantations and agriculture. Deforestation has a strong relationship with changes in rainfall patterns in the area, and this has an impact on the frequency of floods [39]. Many types of vegetation, including shrubs, have also been utilized for agricultural extensification and the extension of housing areas [40], thereby disrupting the balance of the regulation of runoff velocity and water interception [41].

Some areas that were once covered by vegetation have developed into residential areas due to the increase in the human population and the increase in infrastructure building and roads connecting other infrastructures [29,42,43]. The problem that arises due to urbanization and infrastructure development is creating an area or surface that is impermeable to water [14,42]. Such a surface inhibits infiltration after it rains [43]. This changes the water infiltration into the soil and causes an increase in surface overflow, which often results in flooding [44–46].

Information on LULC, drainage patterns, distances from residential areas to water surfaces, elevation, buffers, cultural practices, and attitudes is needed to identify flood-prone areas. Reducing flood risk depends on the knowledge and understanding of the nature of the available physical space and historical data. Therefore, modern techniques are needed in flood mitigation. GIS-based and remote sensing data offer effective tools for processing this information. Many studies on LULCC affect flooding [47–50]. Datasets from Landsat images are then input into the GIS platform to create susceptibility maps. In [47], a flood vulnerability study was conducted in Pordenone Province following major floods. The study confirmed that flooding occurs due to increasing population growth and urbanization, reducing the percentage of natural vegetation. In [51], a study was conducted in the Philippines, concluding that mining with large land clearing, logging, and agricultural expansion using the rip and burn method results in the denudation of watersheds, thereby weakening the ability of the soil to prevent flash floods, while increased soil erosion is characterized by the silting of the river [52]. According to [53], anthropogenic activities, such as increasing residential areas, developing economic and supporting infrastructure in floodplains, and decreasing water holding rates over land use changes, cause an increase in flood occurrence and a decrease in available space.

Much of the information about frequent flooding in the Krueng Teunom watershed is still based on assumptions. The absence of definite information based on research findings on the sources of flooding is dependent on the accuracy and depth of available information regarding the factors causing flooding, such as increasing LULCC and the identification of flood-prone areas [54]. Many locations in this watershed are prone to flooding but have not been well mapped. This study is very important because it utilizes GIS-based and technology advances to produce data in flood hazard maps and identify all flood-prone areas. Therefore, this study aims to examine the extent and characteristics of land cover and land use changes, determine the infiltration capacity, and create a flood risk map for the Krueng Teunom watershed. This information will be useful for policymakers and planners in regional development planning. These results are also important in hazard zoning, early warning, and flood evacuation systems

2. Study Area

The Teunom watershed is located in the Aceh Jaya regency of Aceh Province, Sumatra Island, Indonesia, approximately ~190 km west of Banda Aceh, the capital of Aceh Province. The Teunom watershed is the primary fluvial system in the Aceh Jaya area, with an area of 310.62 km² [10,55]; it is located at 4°26′00.94″ N to 4°44′09.60″ N and 95°48′17.31″ E to 95°59′06.80″ E; and its tip is near the border area of the Pidie regency (Figure 1).

The Krueng Teunom watershed is the main fluvial system in the Aceh Jaya, Aceh Province, Sumatra Island, Indonesia (Figure 1). Krueng Teunom is a river that flows in the Krueng Teunom watershed. The area comprises temperate tropical rainforests, with an average annual temperature of 23 °C. The hottest month is February, with an average temperature of 26 °C, and the coldest is January, which is approximately 22 °C. The average annual rainfall is 4059 mm. The month with the highest rainfall is November, with an average of 536 mm, and the month with the lowest rainfall is July, with an average of 205 mm [56]. The study area is located in the Teunom district, with a total area of 141 km² and a total population of 13,628 in 2021) [57].

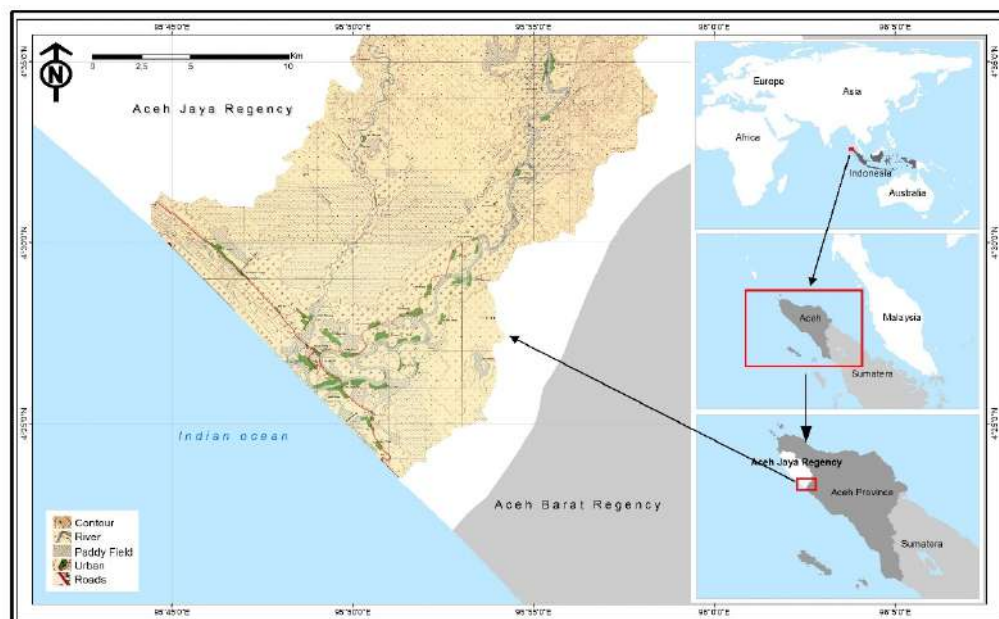


Figure 1. Map of the study area in the Krueng Teunom watershed.

3. Methods

3.1. Research Design

This research used multi-temporal images, topographic maps, soil data, and the Digital Elevation Model (DEM) of the location to perform spatial analysis in a GIS-based mapping tool. We selected different land use types, e.g., residential areas, agricultural land, rice fields, forests, shrubs, and plantations, for the field infiltration sample tests to achieve the research objectives. First, Krueng Teunom drainage data were obtained through identification using 30 m DEM using ArcGIS 10.3 spatial analysis. Furthermore, the watershed was described and analyzed to determine the direction of flow and accumulation flow. This watershed was further digitized and combined with satellite imagery to produce LULC maps and land cover statistics. Thematic maps of land cover, soil type and distribution, and slope were overlaid and analyzed to produce a flood risk map for the study area. Figure 2 provides a summary of the methodology of data collection in the form of a flow chart, which was used for data processing and presentation.

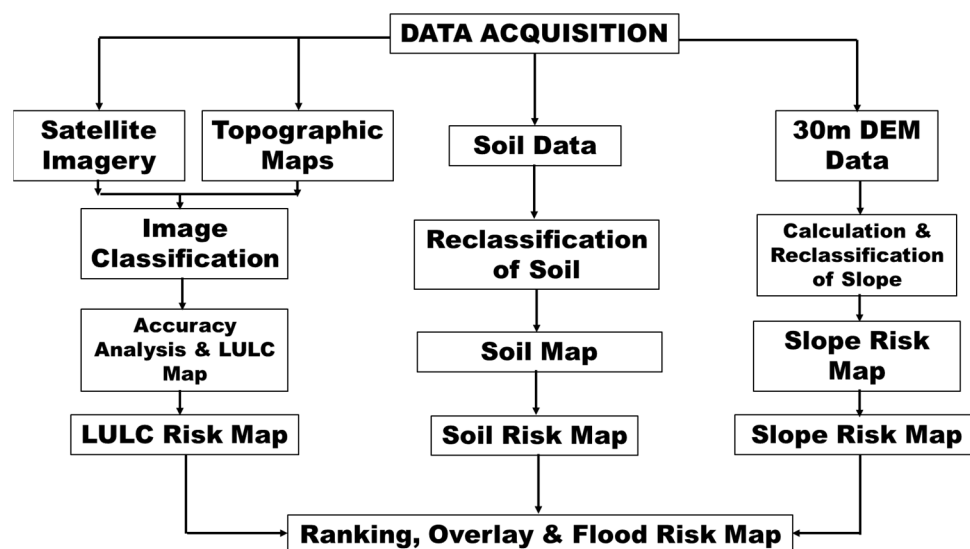


Figure 2. Flow model and research design.

3.2. Data Types, Sources, and Analysis

The data used in this study are primary data and secondary data. The primary data were collected from the field, such as infiltration measurements, sampling points using the Global Positioning System (GPS), and direct field surveys to record land cover. The secondary data were obtained from literature documents, journals, and strategic plans.

3.2.1. Data Sampling

Sampling refers to the population representative method with reference to stratified, purposive, and simple random samples based on each characteristic or type of land cover. The field data collection involved the incorporation of three sampling methods because they were interdependent. The areas were grouped in reference to land cover and land use type (Table 1). Land cover information was collected randomly, and purposive sampling was used to identify locations for infiltration data collection.

Table 1. Description of land use types in the study area.

Land Cover Type	Description
Water body	Dams, pans, seasonal/permanent rivers, ponds, marshy areas, reservoirs
Forest	Primary forests, plantations, forest production areas, mangroves, swamp forests, closed canopies
Bare lands	Large tracks of uncultivated land with scattered trees used for grazing and replanting the estate
Urban	Villages, commercial/residential structures, paved surfaces, roads
Croplands	Planted crops, irrigated crops, perennial crops
Paddy field	Irrigated paddy fields, seasonal paddy fields, swamp paddy fields
Shrublands	Trees/bushes with a height of five feet or less, open or closed canopy

3.2.2. Remote Sensing Data

The 30 m spatial resolution and six-year interval of Landsat 7 Enhanced Thematic Mapper Plus (ETM+) and Landsat 8 Operational Land Imager (OLI) contained eight spectral bands, including a pan and thermal band of path 130, dan 131, and row 057, which were utilized to create LULCC information for 2009, 2013, and 2019. This satellite dataset was obtained through the United States Geological Survey (USGS) official website: <https://www.usgs.gov/> (accessed on 20 April 2022) [58], and the rectified base map of the study area was obtained from the Indonesian Geospatial Data Center [59]. Landsat imagery selection was based on the cloudlessness, clarity, and availability of the selected years of the study area.

3.2.3. DEM Data

DEM data were obtained from the Geospatial Information Board of Indonesia, BIG DEMNAS [60]. The information extracted from DEM included the elevation, the river pattern of the watershed, and water basins in the study area to help define the flow and storage direction (Figure 3). The generated DEM map of the study area was then reclassified to produce the slope angle and flow velocity, which were superimposed to create a flood hazard map of the study area.

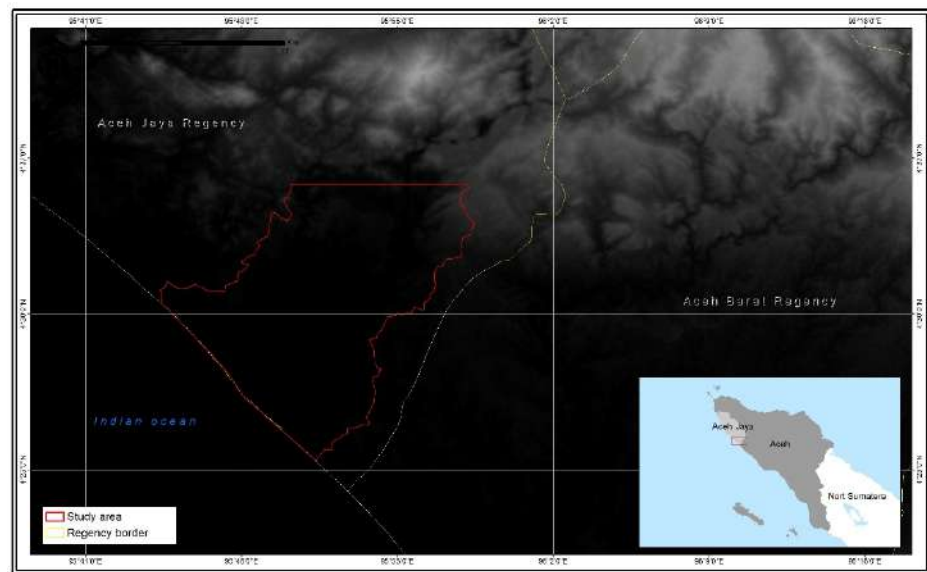


Figure 3. DEM of the study area and surroundings of Teunom watershed.

3.2.4. Soil Data

The soil property information obtained from the Aceh Energy and Mineral Resources Office included soil types, rock formation, and geology. The soil type that refers to soil texture to identify the infiltration capacity of the Teunom watershed consists of clay, loamy sand, sandy loam, and sand. Geologically, the Teunom area consists of tertiary sediment and volcanoes as part of the pre-tertiary continental basement of Sumatera [61]. From the land system point of view, the Teunom watershed consists of plains, turnways, alluvial valleys, beaches, mountains, hills, swamps, and terraces; the land system is dominated by alluvium of the young river, peat, and marine deposit, occupying ~62.56% of the area; the rest consists of conglomerate, basalt, diorite, fine-grained tephra, and coarse-grained tephra [62]. Each soil type is characterized by a different permeability, porosity, and infiltration capacity and therefore has different effects on flooding. These properties are essential to evaluating flood hazards in the study area.

3.2.5. Infiltration Data

Infiltrations data were collected from the field measurements using a double-ring infiltrometer for different land cover types [63]. The calculation was based on the Horton equation model [64]. Seven infiltration data collections were carried out in the study area according to the type of land cover; each assessment of land cover was carried out at three points randomly based on the availability of water and the accessibility of the study area. The infiltration rate was calculated based on the type of land cover, which was tabulated and analyzed using an infiltration curve based on the relationship between infiltration capacity and time.

3.2.6. Land Use Change

The LULC area was calculated for the analysis, and outputs were compared based on different classes. A supervised classification method with a maximum likelihood algorithm was applied to Landsat imagery [49,65]. The overall Cohen's Kappa classification accuracy was 84.00%. The classified images of three other datasets were compared using cross-tabulation to determine the qualitative and quantitative aspects of the changes in 2009, 2013, and 2019. These changes were analyzed based on changes in the area and the

percentage, trend, and rate of change in 2009, 2013, and 2019. Statistics were tabulated and used to calculate the percentages of trend changes using the following formula:

$$\% \text{ of change} = \frac{\text{difference in change} \times 100\%}{\text{Total change}}$$

3.3. Creating Flood Risk Map

The flood risk map was created based on the information reclassified by the land cover and land cover type, soil type, and slope of the study area to identify the spatial resolution of land slopes and soil types [66]. A weighted overlay was employed to construct a flood risk map. A weighted overlay is a spatial analysis method using the GIS tool. The process is based on overlaying two or more base maps with certain weights to create a final map. This method allows problems with many criteria to be solved to determine a location with a particular potential using digital mapping.

3.3.1. Flood Risk Zoning Based on LULC

LULC plays a vital role in water percolation, the infiltration rate, and groundwater recharge. The 2019 land cover map was created with seven land cover classes (Table 1). The classes were then recategorized, weighted, and ranked based on their ability to hold water that ultimately becomes flooded. Settlements were given the highest rating because human intervention affects the soil structure and infiltration capacity through vegetation removal, urbanization, and cultivation. Wetlands were rated the lowest because they act as water absorbers during both dry and rainy seasons.

3.3.2. Flood Risk Zoning Based on Soil Type

Soil type and distribution are the main factors that control the quantity of waterlogging. Different types of soil have the capacity to affect infiltration differently. Soil types were identified and reclassified based on their impact on flood risk. Areas with clay soil types were rated as very risky because they have poor porosity and are less permeable, while sandy soils were considered to have a low flood risk due to their porosity and high permeability.

3.3.3. Flood Risk Zoning Based on Slope

Slope is a significant factor in identifying flood-prone zones. The slope angle affects the speed and frequency of runoff, as well as the rate of infiltration, in an area. On gentle slopes, the runoff is slow; thus, accumulating large amounts of water after a precipitation event tends to result in flooding, whereas on steep slopes, the runoff velocity is high, which allows very little time for water to reside and thus a very small probability of flooding.

The Spatial Analyst Tool in ArcGIS was utilized to compute the slope angle of the DEM. The slope angle was then reclassified to create five classes. The area of the 0.0–5.5% slope was relatively flat and was considered to have the highest flood risk. Areas above 30% had the steepest slope and were considered to have the lowest flood risk. The resulting class was then ranked depending on its effect on flooding.

4. Results and Discussion

4.1. Spatial and Temporal Land Cover Change

The results of the field data collection (Figure 4) show that the geomorphology of the Krueng Teunom watershed is mostly a flat alluvial plain with a gentle slope. The results show that 67% of the Krueng Teunom watershed is an area less than 100 m above sea level. Only approximately 8% of this watershed is an area with an altitude between 250 and 400 m.

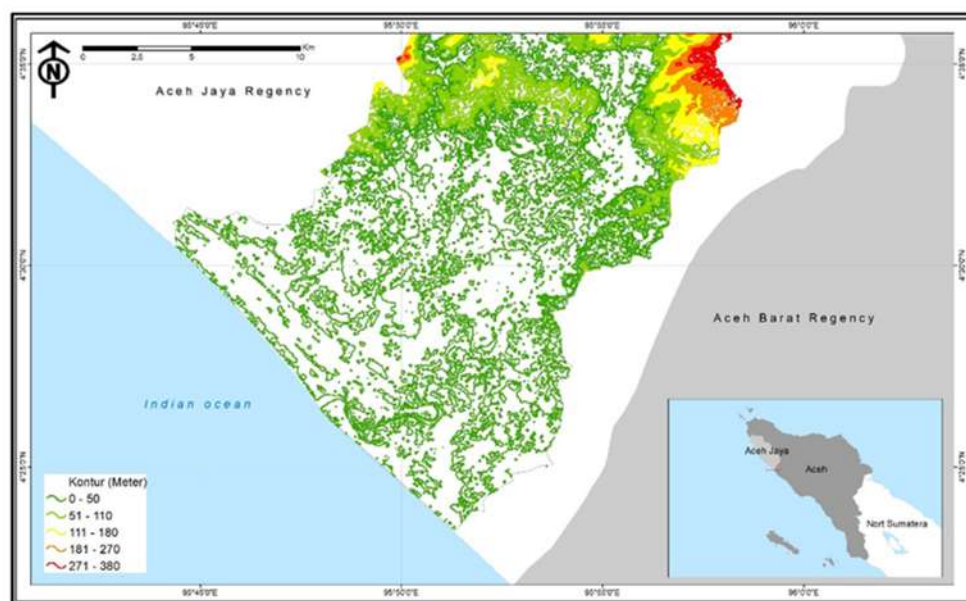


Figure 4. Geomorphological map of the Teunom watershed (combination of field survey results and geospatial data).

The results of the Landsat imagery of the Krueng Teunom watershed were classified into seven main classes, namely, (1) water bodies, (2) forests, (3) open land, (4) settlements, (5) agricultural/plantation land, (6) rice fields, and (7) shrubs. The land use map classification was carried out for ten different years from 2009 to 2019 in three different timescales: 2009, 2013, and 2019 (Table 2). For verification, the multispectral classification was carried out on Landsat images, Google maps, and field surveys. The result of the absolute change in land use was obtained from the difference in the number of cells, and the percentage change was calculated, as shown in Table 2.

Table 2. Land cover change data from 2009 to 2019.

No	Land Cover	2009		2013		2019	
		km ²	%	km ²	%	km ²	%
1.	Water Body	6.61	2.13	6.46	2.08	11.01	3.54
2.	Forest	57.61	18.55	63.80	20.54	54.51	17.55
3.	Bare lands	0.37	0.12	0.63	0.20	2.56	0.82
4.	Urban	2.59	0.83	4.04	1.30	5.55	1.79
5.	Croplands	193.23	62.21	204.97	65.99	190.46	61.31
6.	Paddy field	2.93	0.94	3.18	1.02	19.36	6.23
7.	Shrublands	47.29	15.22	27.53	8.86	27.17	8.75
Total		310.67	100.00	310.67	100.00	310.67	100.00

The land use statistics for the Krueng Teunom watershed reveal changes in all land uses in this area. This analysis result was achieved through the comparison of land use between 2009 and 2019. Figure 5 shows the land use map obtained after classification. Shrubland almost tripled after 2009, with an average increase of 0.21 km² per year. Forests, based on data in 2013, increased by 2%; then, in 2019, they decreased by approximately 3%, indicating forest conversion for rice fields and residences due to population growth [67]. This also occurred in agricultural land cover, which decreased by 5% or approximately 14 km² after 2013. The initial residential area of 2.59 km² in 2009 increased to 5.55 km² or approximately 100% in 2019, with an average annual land use growth rate of 0.3 km². Rice fields, on the other hand, which were originally 2.93 km² in 2009, increased to 19.36 km² in 2019, with an average annual land use growth rate of 1.6 km² per year. Meanwhile, the water body, which, in 2009, was only 6.61 km², increased by 11.01 km², with an increase of

0.4 km² per year. If it is assumed that the growth rate of residential land use in the Krueng Teunom area is constant at 0.3 km² per year, then, in 2025, this area will occupy 4.77 km², which is approximately 1.5% of the total watershed area.

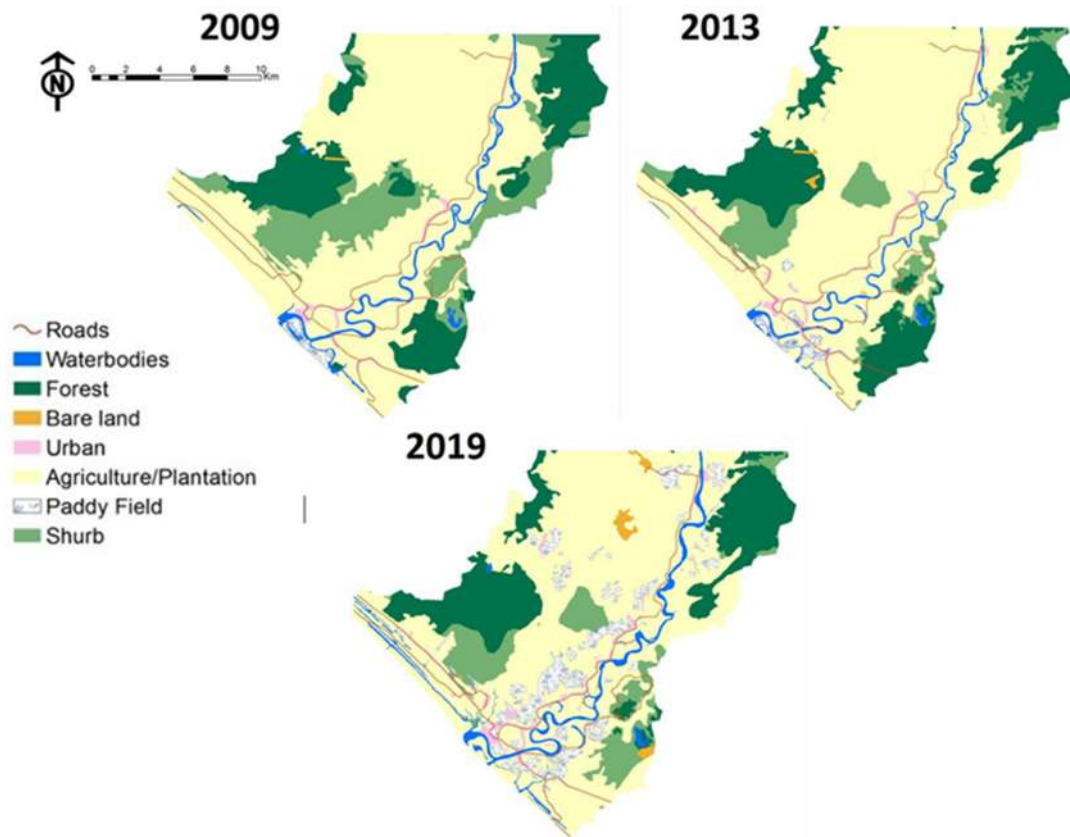


Figure 5. Spatial map of Krueng Teunom watershed land use from 2009 to 2019.

The results of the land cover analysis (Table 2) based on survey results combined with geospatial data show that the Krueng Teunom watershed experienced significant degradation when compared to geospatial data in 2009 and 2013 (Figure 6). The greatest change occurred in the conversion of scrubland into rice fields due to the increase in population. Scrubland conversion is easy to do in rice fields. Part of the forest land is turned into water bodies in low-lying areas, while plantation land is used for settlement expansion. As a result, the open land is expanding, causing the hydrological water capacity to shrink. This can be seen from the increasing magnitude of water bodies due to silting as a result of erosion from the watershed land.

Land cover characteristics changes are important to analyze the level of flood risk in an area. This increase is linear with the increase in the residential area, which indicates an increase in the number of residents [68]. This will indirectly increase the number of people vulnerable to flooding. The exposure to flood risk in developing residential areas will be accelerated by increasing spatially impermeable land and changes in natural drainage channels [69]. This is due to the inhibition of water infiltration after a precipitation event, which is a contributing factor to flooding.

The increase in population resulted in increased food consumption, resulting in an increased use of agricultural land at the expense of forest land, shrubs and bare lands, most of which function as flood plains [70]. During the flood event, most of the agricultural land was covered by water, causing crop and economic losses. These events put the people living in the area, which is their main source of livelihood, at risk of starvation. The continuous plowing of agricultural land will also loosen the soil, thereby increasing the possibility of riverbed sedimentation as the topsoil is carried away by water [71]. Sedimentation

at the bottom of the river will raise the water level in the river, which also increases flooding [10,71].

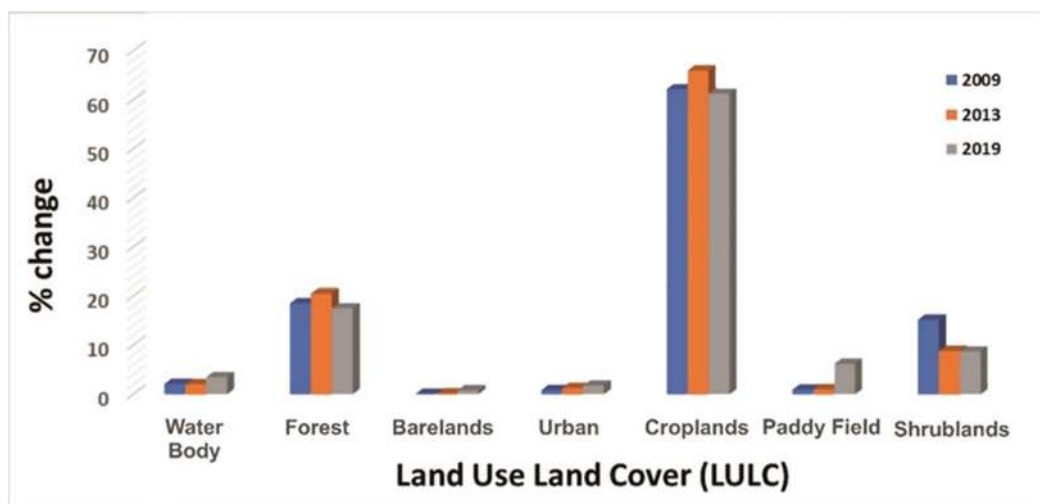


Figure 6. Results of land use analysis for the Krueng Teunom watershed in 2009, 2013, and 2019.

4.2. Impact of LULC on Runoff and Infiltration Capacity

The results of the infiltration experiments carried out in each cover class to determine the infiltration capacity can be seen in Table 3. The infiltration experiments in each land class were tested based on water availability and location access. Based on the experimental results, the highest infiltration rate was found in sandy areas, while the lowest infiltration rate was found in clay soil. This explains that the type of soil affects the rate of infiltration [72].

Table 3. Results of infiltration experiments in the field.

No	Land Classification	Water Level Reading (cm)	Time (s)	Infiltration Rate (cm/s)	Soil Type
1.	Agriculture	0.2	240.12	0.000640	Sandy loam
2.	Forest	0.2	240.12	0.000833	Clay
3.	Bare lands	0.0	240.12	0.000000	Clay
4.	Paddy field	0.3	360.00	0.000670	Clay
5.	Urban	0.7	540.00	0.001200	Sand
6.	Shrubs	0.1	420.12	0.000140	Loamy sand

In the field testing, it took approximately 4 min for water to completely infiltrate in agricultural land, which is sandy loam soil, an average of 4 min in forest land, an average of 7 min in bare lands, an average of 6 min in rice fields, an average of 9 min in residential areas, and an average of 4 min in shrubs. For experiments conducted under clay, it took an average of 5.67 min for water to seep into the soil in bare lands and 9 min in residential areas. The results of the water absorption experiment on sandy clay soil types showed an average of 4 min in agricultural land, 4 min in grasslands, and 9 min in residential areas, respectively, while for sandy soil, it took an average of 9 min in residential areas.

The water level readings differed in the experiments carried out as a result of the permeability of the material type located underground and the depth of the soil. Therefore, there was an opportunity for increased flooding as a result of decreased soil infiltration capacity and increased runoff. During precipitation, the absorption of water by the soil can exceed the ability of the soil to absorb water; therefore, if soil infiltration decreases, the possibility of flooding will occur more quickly.

In residential areas, the land is mostly paved and cemented so that it is impermeable to surface water. The soil surface that is modified to be hard takes a lot of time to seep

into the soil when it rains [73]. Most of the rainfall in residential zones flows in the form of runoff, accumulates in low land areas, has an impact on water absorption, and causes flooding [74]. According to [75], runoff velocity is highest in residential areas due to the difficulty of water seeping into the ground; hence, most of the water uses canals to flow to other low land, often at a high speed and in a great volume. As a result, the accumulation of water in low land areas will cause flooding and erosion. This also occurs in rice fields, where infiltration also has a low value due to soil compaction during land cultivation and weeding. Generally, the paddy fields in the Krueng Teunom watershed are highly mechanized agricultural lands with a higher soil density due to its low infiltration rate and large runoff velocity.

Forest and scrubland areas were found to have high water infiltration rates and low runoff rates. This is caused by the trees and leaves in this area reducing the runoff rate of water when it rains such that the erosion effect due to the speed of erosion by water is significantly reduced, so it has more time to absorb water [76]. On the other hand, the level of infiltration in the shrubs was found to be moderate because the shrubs, which also contain grass, also block water runoff and give the water time to be absorbed into the soil.

4.3. Flood Risk Zoning

Several key factors are considered to produce a flood risk zoning, especially physical parameters such as land cover characteristics; soil types that affect infiltration; and topography (elevation and slope), hydrology (drainage), and rainfall. The following is a description of flood hazard zoning based on the land cover distribution, elevation, and slope of the watershed and soil type.

4.3.1. Based on Land Cover Distribution

Land cover characteristics not only affect land use but also affect soil infiltration and soil stability [77]. Vegetation, such as forests, grasslands, shrubs, and even food crops on agricultural land, has an impact on the capacity of the soil to reduce runoff, thereby reducing the amount of flooding water on vacant land or land with a low infiltration rate, i.e., impermeable land such as residential areas.

The analysis used to determine the risk of flooding due to land cover distribution used a map of the distribution of land cover in 2019 (Table 2 and Figure 5). It was possible to identify the inhabitation areas in residential areas, and they were least likely to be found in swampy areas. In many cases, drainage canals and culverts in residential areas are usually too small to accommodate rainwater, which causes water to overflow in residential areas. This problem is exacerbated by the large amount of solid waste that is dumped in the open by residents, clogging the drainage system. Land cover appearances and land use activities thus only add to the flood risk posed by the infiltration capacity [78], as well as the nature of the slopes on which the land use activities are carried out. The geology of the area under each LULC category is due to its effect on soil infiltration and runoff [72,76]. Changes in LULC, especially the removal of vegetation, increase the chance of the area being at risk of flooding [79].

In accordance with the obtained results (Figure 7), it can be said that the reduction in grassland/shrubs increases the water discharge. Therefore, grasslands/shrubs are equally important in controlling river discharge when rainfall increases. Vegetation (forests and shrubs) plays an important role in reducing peak water discharge loads [80]. Watersheds with vegetation gradually restrain the speed of water discharge so that the peak load increases gradually; on the other hand, watersheds without vegetation will increase the discharge rate sharply and suddenly [81]. This shows that lands that have an effect on reducing water infiltration, when precipitation occurs in the watershed, will be quickly converted into runoff, which ends up in basins and rivers. Therefore, the accumulation of water volume builds up quickly, while the capacity is small, causing water runoff and flooding.

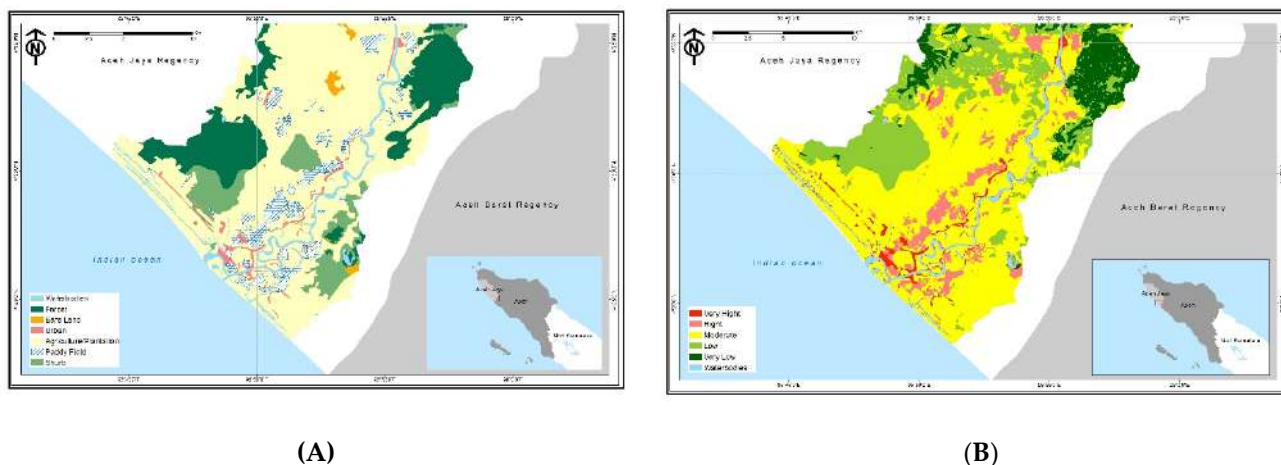


Figure 7. Land cover characteristics in relation to flood risk occurrence: (A) land use–land cover condition and (B) flood risk map.

4.3.2. Based on the Distribution of Elevation and Slope

The survey results explain that the Krueng Teunom watershed is geologically an alluvial deposition area, with the dominant sediment originating from the Miocene era (results of a field survey). Geomorphologically (Table 4, Figures 1 and 8), the Krueng Teunom watershed is a low-lying area with a slope of 0.0–5.5%, covering an area of approximately ~85% of the watershed area; the rest are upland and mountainous areas that have slopes greater than 5.5%, occupying an area of ~14%. In lowland areas, ~67% of the total area is rice fields and agriculture, and the rest is plantation areas and a small portion of forests and water bodies.

Table 4. Classification of the slope of the Krueng Teunom watershed and its coverage area.

No	Slope Angle	Area (km ²)	% Area
1.	0.0–1.2	132.194	42.56
2.	1.2–3.0	105.944	34.11
3.	3.0–5.5	27.665	8.91
4.	5.5–10.3	33.030	10.63
5.	10.3–30.0	11.780	3.79
6.	>30.0	0.001	0.00
Total		310.620	100.00

The results of the topographic map analysis show that most of the Krueng Teunom watershed area is a sloping plain with a very high risk of flooding in the event of inundation due to rain, while steep slopes have a small area, so they have a very small risk of flooding because the overflow water moves at a relatively high speed. The rest are areas of moderate steepness that have a moderate risk of flooding.

The slope map in this study was compiled from the DEM of the Krueng Teunom watershed. The class of each slope was graded from a low-risk class to high-risk class. Classes with steep slope values were rated as being at a low risk of flooding. Such areas do not allow for the accumulation of water build-up, which, in turn, causes waterlogging [82]. The greatest flood risks are in areas that are flat; have soils with a low infiltration capacity, such as clay and loam; are poorly drained; do not have vegetation; and have land use activities within them that prevent percolation, especially in residential areas (Figure 8).

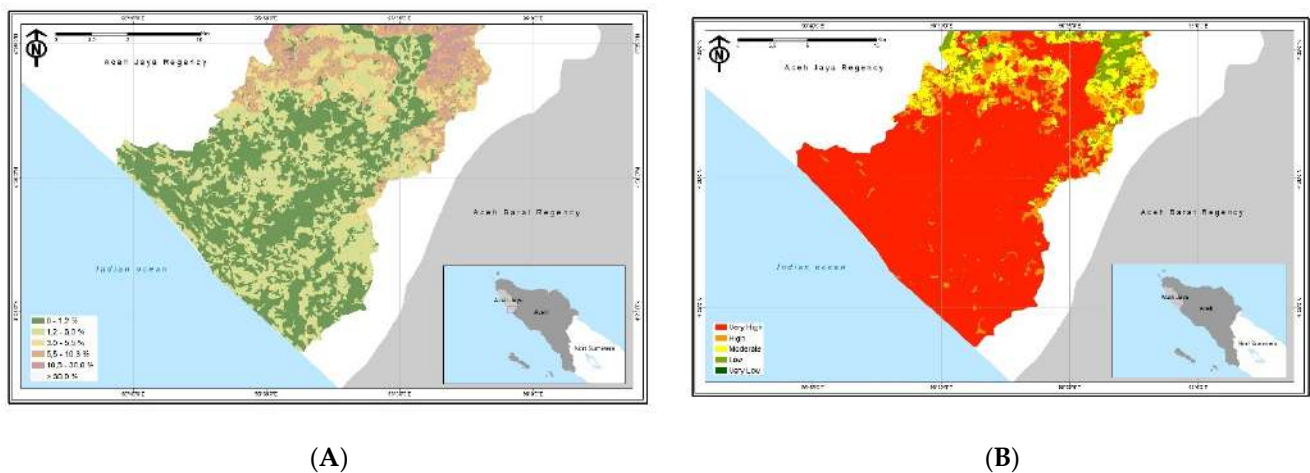


Figure 8. Topographic map (elevation and slope) of Krueng Teunom and its relation to flood disasters: (A) elevation and slope map and (B) flood risk map.

4.3.3. Based on Soil Type Distribution

The soil classification in this study was based on the type of surface soil in the Krueng Teunom watershed, which is categorized into four types, namely, clay, sandy clay, loamy sand, and sand (Table 5). Meanwhile, the distribution of the soil types can be seen in Figure 9. The classes of soil types were classified into three main classes of flood risk levels. A high value was assigned the number “3”, while the type of soil with the least possibility of flooding was given a rating of “1”.

Table 5. Classification of soil types and area of cover.

No	Soil Type	Soil Flood Risk	Area (km ²)	% Area
1	Clay	High	20.075	42.56
2	Loamy sand	High	28.167	34.11
3	Clay	Low	56.515	8.91
4	Sandy loam	Moderate	197.452	0.63
5	Clay	Very high	2.650	3.79
6	Sand	Very high	5.757	0.00
Total			310.62	100.00

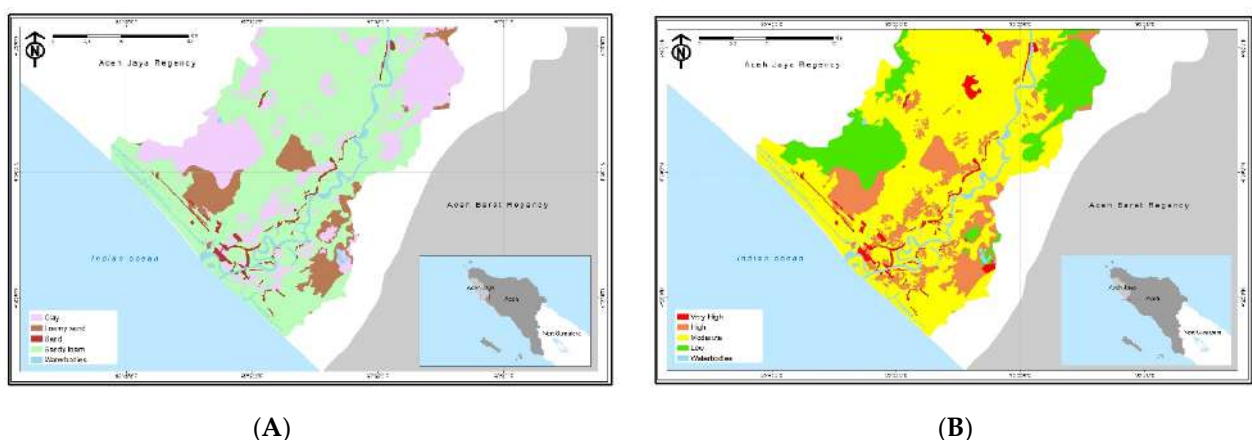


Figure 9. Soil type map (A) and soil flood risk map (B) of Krueng Teunom watershed.

Soil texture greatly affects the level of flood risk. Sandy soil types produce high infiltration and permit water to pass through faster than other soil types. Sandy soils have

soil particles and large soil pores, so they are able to absorb water faster and, thus, runoff is small, while the type of clay, besides having fine particles, is also less permeable as a result of less soil absorption and a large runoff, so it accumulates water for a longer period of time. This type of soil restrains the rate of water infiltration into the soil such that it retains water, and the implication is that it is vulnerable and more likely to be at risk of flooding. Other important factors when evaluating the impact of soil type on flooding are soil structure and infiltration capacity. Therefore, different soil types have different infiltration capacities; if the infiltration capacity is low, then the risk of flooding is more likely to occur [83].

4.4. Flood Risk Map

The flood risk area map was generated from a combination of thematic maps overlaid using spatial analysis in ArcGIS. The resulting outputs were four flood risk classes from low to very high (Table 6 and Figure 10). The results of the analysis showed that the high-flood-risk zone covers the widest area. The very-high-risk zone is concentrated on the south side of the area and in the coastal area. These areas are the main residential areas according to the land use map classification (Figure 7). These areas are mostly characterized by clay with flat elevations and gentle slopes (Table 7). This risk area is also located along the coastline, facing the risk of coastal flooding due to its proximity to the sea. Most areas of agricultural land and grasslands are also included in the high-risk zone of flooding.

Table 6. Classification of flood risk and area of land cover.

No	Risk Classification	km ²	% Area
1	Very Low	29.758	9.58
2	Low	68.97	22.21
3	Moderate	174.69	56.24
4	High	21.64	6.97
5	Very High	15.56	5.01
		310.62	100.00

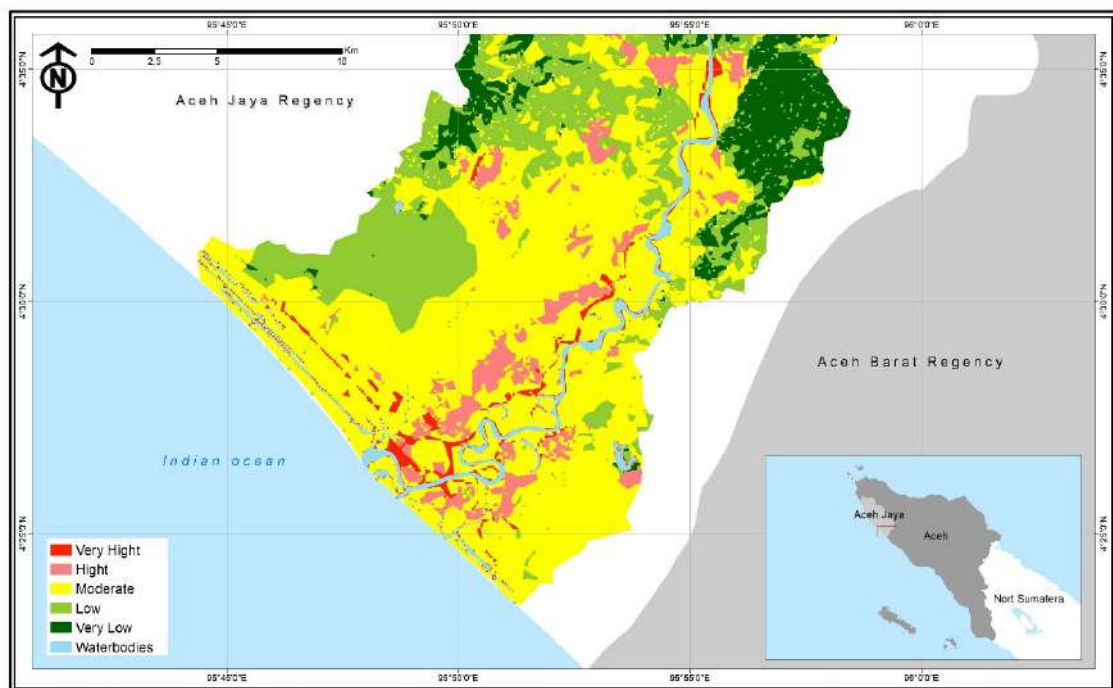


Figure 10. Overlaid flood risk map results from the overall analysis.

Table 7. Flood risk class based on different slopes of Krueng Teunom watershed and its coverage area.

No	Flood Risk	Slope (%)	Area (km ²)	% Area
1	Very high	0.0–1.2	132.12	42.56
2	Very high	1.2–3.0	105.88	34.11
3	High	3.1–5.0	27.65	8.91
4	Moderate	5.5–10.3	33.01	10.63
5	Low	10.3–30.0	11.77	3.79
6	Very Low	>30.0	0.00	0.00
Total			310.43	100.00

5. Conclusions

The expansion of residential land and changes in open land, paddy fields, and wetlands (bodies of water) due to unbalanced land use has led to an increase in the incidence of flooding due to soil saturation and affects the infiltration capacity of the soil. Changes in land use also change the water runoff and river discharge due to siltation on the river and water body. The spatial analysis results of land use, soil type, and slope indicated that the Teunom watershed has a high and very high risk of ~11.98% of the total area, a moderate risk of 56.24%, and a low and very low risk of ~31.79% of the total area. Thus, the Teunom watershed generally has a high flood risk, which makes the overall risk of flooding in the area moderate to very high, with a total of ~68% of the total area. Therefore, the segmentation of flood-risk zones is essential for development preparation in the study area. This study offers necessary information about flood hazard areas for central governments, local governments, NGOs, and communities to intervene in preparedness, responses, and flood mitigation and recovery processes if flooding occurs.

Author Contributions: Conceptualization, S.S. and M.I.; methodology, M.R.; software, S.S. and M.R.; validation, E.M.; formal analysis, S.S., M.I. and M.R.; investigation, M.I., A.D. and E.M.; resources, M.R.; data curation, M.R. and A.D.; writing—original draft preparation, S.S. and M.I.; writing—review and editing, E.M. and A.D.; visualization, M.R.; supervision, S.S. and M.I.; project administration, S.S. and A.D.; funding acquisition, S.S. All authors have read and agreed to the published version of the manuscript.

Funding: This research received no external funding.

Institutional Review Board Statement: Not applicable.

Informed Consent Statement: Not applicable.

Data Availability Statement: All the data generated or analyzed during this study are included in this article.

Acknowledgments: All authors gratefully acknowledge to Pusat Penelitian dan Pengabdian Kepada Masyarakat (LPPM) universitas Syiah Kuala for their financial support.

Conflicts of Interest: The authors declare no conflict of interest.

References

1. Yenni; Helmi; Hermansah. Hydrologic Characteristics, Flood Occurrence, and Community Preparedness in Coping With Floods at Air Dingin Watershed, Padang, West Sumatra. In *Redefining Diversity & Dynamics of Natural Resources Management in Asia*; Elsevier: Amsterdam, The Netherlands, 2017; Volume 4, pp. 157–172.
2. Kadri, T.; Kurniyaningrum, E. Impact of Land Use on Frequency of Floods in Upper Bekasi Watershed, Indonesia. *Int. J. Sci. Technol. Res.* **2019**, *8*, 3328–3334.
3. Narulita, I.; Ningrum, W. Extreme flood event analysis in Indonesia based on rainfall intensity and recharge capacity. *IOP Conf. Ser. Earth Environ. Sci.* **2018**, *118*, 012045. [[CrossRef](#)]
4. Wells, J.A.; Wilson, K.A.; Abram, N.K.; Nunn, M.; Gaveau, D.L.A.; Runting, R.K.; Tarniati, N.; Mengersen, K.L.; Meijaard, E. Rising floodwaters: Mapping impacts and perceptions of flooding in Indonesian Borneo. *Environ. Res. Lett.* **2016**, *11*, 064016. [[CrossRef](#)]
5. Faradiba, F. The Impact of Climate on Flood Disasters in Indonesia. *Int. J. Progress. Sci. Technol.* **2022**, *31*, 364–371.

6. Lestari, S.; King, A.; Vincent, C.; Karoly, D.; Protat, A. Seasonal dependence of rainfall extremes in and around Jakarta, Indonesia. *Weather Clim. Extrem.* **2019**, *24*, 100202. [[CrossRef](#)]
7. Supari, S.; Ettema, J.; Aldrian, E. Spatio Temporal Characteristic of Extreme Rainfall Events over Java Island, Case: East Java Province. *Indones. J. Geogr.* **2012**, *44*, 62–86. [[CrossRef](#)]
8. Ambari, L.W. Indonesia Suffers Sixty Floodings in a Decade. Available online: <https://bali.antaranews.com/berita/38426/indonesia-suffers-sixty-floodings> (accessed on 27 July 2022).
9. Bahri, S. Banjir Luapan di Aceh Jaya belum Surut. Available online: <https://aceh.tribunnews.com/2016/10/17/banjir-luapan-di-aceh-jaya-belum-surut> (accessed on 22 July 2022).
10. Irham, M.; Ilhamsyah, Y.; Sugianto; Deli, A.; Syahreza, S. Is flash flood cycle? A preliminary climate study on Teunom fluvial system. *IOP Conf. Ser. Earth Environ. Sci.* **2019**, *273*, 012001. [[CrossRef](#)]
11. BPDB, A. *Laporan Penanggulangan Banjir Provinsi Aceh*; PEMDA Provinsi Aceh: Banda Aceh, Indonesia, 2016.
12. PEMDA, A.J. *Rencana Strategis*; PEMDA Aceh Jaya: Calang, Indonesia, 2016.
13. Irham, M. The Spatial Distribution of Bed Sediment on Fluvial System: A Mini Review of the Aceh Meandering River. *Aceh Int. J. Sci. Technol.* **2016**, *5*, 82–87. [[CrossRef](#)]
14. Irham, M.; Irpan, M.; Sartika, D.; Setiya Nugraha, G.; Dharma, D.B. Study of the suitability of rock type with the chemical topology of groundwater in the Jeunib basin, Aceh. *Arab. J. Geosci.* **2022**, *15*, 220. [[CrossRef](#)]
15. Griffiths, M.L.; Drysdale, R.N.; Gagan, M.K.; Zhao, J.X.; Ayliffe, L.K.; Hellstrom, J.C.; Hantoro, W.S.; Frisia, S.; Feng, Y.X.; Cartwright, I.; et al. Increasing Australian-Indonesian monsoon rainfall linked to early Holocene sea-level rise. *Nat. Geosci.* **2009**, *2*, 636–639. [[CrossRef](#)]
16. Meilianda, E.; Alfian, D.; Nisa, N.; Nurnalisa, F.Z.; Khaira, T.; Yanti, V.; Syahreza, S. Tinjauan Teknis Permasalahan dan Penanggulangan Banjir di Sungai Krueng Teunom Hilir Provinsi Aceh, Menuju Mitigasi Bencana Banjir Terintegrasi. *J. Tek. Sipil* **2021**, *28*, 51–62. [[CrossRef](#)]
17. Loc, H.H.; Park, E.; Chitwatkulsiri, D.; Lim, J.; Yun, S.H.; Maneechot, L.; Minh Phuong, D. Local rainfall or river overflow? Re-evaluating the cause of the Great 2011 Thailand flood. *J. Hydrol.* **2020**, *589*, 125368. [[CrossRef](#)]
18. Meyers, S.D.; Landry, S.; Beck, M.W.; Luther, M.E. Using logistic regression to model the risk of sewer overflows triggered by compound flooding with application to sea level rise. *Urban Clim.* **2021**, *35*, 100752. [[CrossRef](#)]
19. Sholihah, Q.; Kuncoro, W.; Wahyuni, S.; Puni Suwandi, S.; Dwi Feditasari, E. The analysis of the causes of flood disasters and their impacts in the perspective of environmental law. *IOP Conf. Ser. Earth Environ. Sci.* **2020**, *437*, 012056. [[CrossRef](#)]
20. Gan, B.R.; Liu, X.N.; Yang, X.G.; Wang, X.K.; Zhoua, J.W. The impact of human activities on the occurrence of mountain flood hazards: Lessons from the 17 August 2015 flash flood/debris flow event in Xuyong County, South-Western China. *Geomat. Nat. Hazards Risk* **2018**, *9*, 816–840. [[CrossRef](#)]
21. Vaezi, A.R.; Bahrami, H.A.; Sadeghi, S.H.R.; Mahdian, M.H. Modeling relationship between runoff and soil properties in dry-farming lands, NW Iran. *Hydrol. Earth Syst. Sci. Discuss.* **2010**, *7*, 2577–2607. [[CrossRef](#)]
22. Huang, J.; Kang, Q.; Yang, J.X.; Jin, P.W. Multifactor analysis and simulation of the surface runoff and soil infiltration at different slope gradients. *IOP Conf. Ser. Earth Environ. Sci.* **2017**, *82*, 012019. [[CrossRef](#)]
23. van Heerwaarden, C.C.; de Arellano, J.V.G. Relative humidity as an indicator for cloud formation over heterogeneous land surfaces. *J. Atmos. Sci.* **2008**, *65*, 3263–3277. [[CrossRef](#)]
24. Srivastava, A.; Kumari, N.; Maza, M. Hydrological Response to Agricultural Land Use Heterogeneity Using Variable Infiltration Capacity Model. *Water Resour. Manag.* **2020**, *34*, 3779–3794. [[CrossRef](#)]
25. Aghsaee, H.; Mobarghaee Dinan, N.; Moridi, A.; Asadolahi, Z.; Delavar, M.; Fohrer, N.; Wagner, P.D. Effects of dynamic land use/land cover change on water resources and sediment yield in the Anzali wetland catchment, Gilan, Iran. *Sci. Total Environ.* **2020**, *712*, 136449. [[CrossRef](#)]
26. Smith, P.; Cotrufo, M.F.; Rumpel, C.; Paustian, K.; Kuikman, P.J.; Elliott, J.A.; McDowell, R.; Griffiths, R.I.; Asakawa, S.; Bustamante, M.; et al. Biogeochemical cycles and biodiversity as key drivers of ecosystem services provided by soils. *Soil* **2015**, *1*, 665–685. [[CrossRef](#)]
27. Zeiger, S.J.; Hubbart, J.A. Quantifying land use influences on event-based flow frequency, timing, magnitude, and rate of change in an urbanizing watershed of the central USA. *Environ. Earth Sci.* **2018**, *77*, 107. [[CrossRef](#)]
28. Maskrey, S.; Mount, A.; Nick, J.; Thorne, C.T. Doing flood risk modelling differently: Evaluating the potential for participatory techniques to broaden flood risk management decision-making. *Flood Risk Manag.* **2022**, *15*, e12757. [[CrossRef](#)]
29. Ganaie, T.A.; Jamal, S.; Ahmad, W.S. Changing land use/land cover patterns and growing human population in Wular catchment of Kashmir Valley, India. *GeoJournal* **2021**, *86*, 1589–1606. [[CrossRef](#)]
30. Rimba, A.B.; Mohan, G.; Chapagain, S.K.; Arumansawang, A.; Payus, C.; Fukushi, K.; Husnayaen; Osawa, T.; Avtar, R. Impact of population growth and land use and land cover (LULC) changes on water quality in tourism-dependent economies using a geographically weighted regression approach. *Environ. Sci. Pollut. Res.* **2021**, *28*, 25920–25938. [[CrossRef](#)]
31. Danandeh Mehr, A.; Akdegirmen, O. Estimation of Urban Imperviousness and its Impacts on Flashfloods in Gazipaşa, Turkey. *Knowl. Based Eng. Sci.* **2021**, *2*, 9–17. [[CrossRef](#)]
32. Das, P.; Behera, M.D.; Patidar, N.; Sahoo, B.; Tripathi, P.; Behera, P.R.; Srivastava, S.K.; Roy, P.S.; Thakur, P.; Agrawal, S.P.; et al. Impact of LULC change on the runoff, base flow and evapotranspiration dynamics in eastern Indian river basins during 1985–2005 using variable infiltration capacity approach. *J. Earth Syst. Sci.* **2018**, *127*, 19. [[CrossRef](#)]

33. da Costa Silva, J.F.C.B.; da Silva, R.M.; Santos, C.A.G.; Silva, A.M.; Vianna, P.C.G. Analysis of the response of the Epitácio Pessoa reservoir (Brazilian semiarid region) to potential future drought, water transfer and LULC scenarios. *Nat. Hazards* **2021**, *108*, 1347–1371. [[CrossRef](#)]
34. Li, X.; Zhang, Y.; Ma, N.; Li, C.; Luan, J. Contrasting effects of climate and LULC change on blue water resources at varying temporal and spatial scales. *Sci. Total Environ.* **2021**, *786*, 147488. [[CrossRef](#)]
35. Sahoo, S.; Dhar, A.; Debsarkar, A.; Kar, A. Impact of water demand on hydrological regime under climate and LULC change scenarios. *Environ. Earth Sci.* **2018**, *77*, 341. [[CrossRef](#)]
36. Nahib, I.; Ambarwulan, W.; Rahadiati, A.; Munajati, S.L.; Prihanto, Y.; Suryanta, J.; Turmudi, T.; Nuswantoro, A.C. Assessment of the Impacts of Climate and LULC Changes on the Water Yield in the Citarum River Basin, West Java Province, Indonesia. *Sustainability* **2021**, *13*, 3919. [[CrossRef](#)]
37. Abdullah, H.M.; Islam, I.; Miah, M.G.; Ahmed, Z. Quantifying the spatiotemporal patterns of forest degradation in a fragmented, rapidly urbanizing landscape: A case study of Gazipur, Bangladesh. *Remote Sens. Appl. Soc. Environ.* **2019**, *13*, 457–465. [[CrossRef](#)]
38. Cazzolla Gatti, R.; Liang, J.; Velichevskaya, A.; Zhou, M. Sustainable palm oil may not be so sustainable. *Sci. Total Environ.* **2019**, *652*, 48–51. [[CrossRef](#)]
39. Kim, S.; Sohn, H.-G.; Kim, M.-K.; Lee, H. Analysis of the Relationship among Flood Severity, Precipitation, and Deforestation in the Tonle Sap Lake Area, Cambodia Using Multi-Sensor Approach. *KSCE J. Civ. Eng.* **2019**, *23*, 1330–1340. [[CrossRef](#)]
40. Hu, Q.; Xiang, M.; Chen, D.; Zhou, J.; Wu, W.; Song, Q. Global cropland intensification surpassed expansion between 2000 and 2010: A spatio-temporal analysis based on GlobeLand30. *Sci. Total Environ.* **2020**, *746*, 141035. [[CrossRef](#)]
41. Oda, T.; Egusa, T.; Ohte, N.; Hotta, N.; Tanaka, N.; Green, M.B.; Suzuki, M. Effects of changes in canopy interception on stream runoff response and recovery following clear-cutting of a Japanese coniferous forest in Fukuroyamasawa Experimental Watershed in Japan. *Hydrol. Process.* **2021**, *35*, e14177. [[CrossRef](#)]
42. Naikoo, M.W.; Rihan, M.; Ishtiaque, M. Shahfahad Analyses of land use land cover (LULC) change and built-up expansion in the suburb of a metropolitan city: Spatio-temporal analysis of Delhi NCR using landsat datasets. *J. Urban Manag.* **2020**, *9*, 347–359. [[CrossRef](#)]
43. Nithila Devi, N.; Sridharan, B.; Kuiry, S.N. Impact of urban sprawl on future flooding in Chennai city, India. *J. Hydrol.* **2019**, *574*, 486–496. [[CrossRef](#)]
44. Astuti, I.S.; Sahoo, K.; Milewski, A.; Mishra, D.R. Impact of Land Use Land Cover (LULC) Change on Surface Runoff in an Increasingly Urbanized Tropical Watershed. *Water Resour. Manag.* **2019**, *33*, 4087–4103. [[CrossRef](#)]
45. Lacher, I.L.; Ahmadisharaf, E.; Fergus, C.; Akre, T.; Mcshea, W.J.; Benham, B.L.; Kline, K.S. Scale-dependent impacts of urban and agricultural land use on nutrients, sediment, and runoff. *Sci. Total Environ.* **2019**, *652*, 611–622. [[CrossRef](#)]
46. Alayani, R.; Sugianto, S.; Basri, H. Flood Rate Assessment of the Woyla River Watershed, Aceh Province, Indonesia. *Aceh Int. J. Sci. Technol.* **2021**, *10*, 84–99. [[CrossRef](#)]
47. Barredo, J.I.; Engelen, G. Land use scenario modeling for flood risk mitigation. *Sustainability* **2010**, *2*, 1327–1344. [[CrossRef](#)]
48. Hua, A.K. Land Use Land Cover Changes in Detection of Water Quality: A Study Based on Remote Sensing and Multivariate Statistics. *J. Environ. Public Health* **2017**, *2017*, 7515130. [[CrossRef](#)] [[PubMed](#)]
49. Rawat, J.S.; Kumar, M. Monitoring land use/cover change using remote sensing and GIS techniques: A case study of Hawalbagh block, district Almora, Uttarakhand, India. *Egypt. J. Remote Sens. Space Sci.* **2015**, *18*, 77–84. [[CrossRef](#)]
50. Liping, C.; Yujun, S.; Saeed, S. Monitoring and predicting land use and land cover changes using remote sensing and GIS techniques—A case study of a hilly area, Jiangle, China. *PLoS ONE* **2018**, *13*, e0200493. [[CrossRef](#)]
51. Antonio, P.; Carandang, L.A.B.; Dolom, P.C.; Garcia, L.N.; Magdalena, M.; Villanueva, B.; Espiritu, N.O. *Analysis of Key Drivers of Deforestation and Forest Degradation in the Philippines*; Deutsche Gesellschaft für Internationale Zusammenarbeit (GIZ) GmbH: Manila, Philippine, 2013.
52. Boardman, J.; Vandaele, K.; Evans, R.; Foster, I.D.L. Off-site impacts of soil erosion and runoff: Why connectivity is more important than erosion rates. *Soil Use Manag.* **2019**, *35*, 245–256. [[CrossRef](#)]
53. Chalise, D.; Kumar, L.; Kristiansen, P. Land Degradation by Soil Erosion in Nepal: A Review. *Soil Syst.* **2019**, *3*, 12. [[CrossRef](#)]
54. Dalanhol, I.; Tabalipa, N.L.; Meireles Silva, F.C. Future Land-use and Land-cover Scenarios for Mapping Flood-prone Areas in Pato Branco City, Brazil. *KnE Eng.* **2020**, *18*, 333–341. [[CrossRef](#)]
55. Gadeng, A.N.; Ramli, R.; Maulidian, M.O.R.; Aksa, F.I.; Rohmat, D.; Desfandi, M. Kajian Tipologi dan Pemanfaatan Sumber Daya Air di Provinsi Aceh. *J. Ilmu Lingkungan.* **2020**, *18*, 333–341. [[CrossRef](#)]
56. Badan Metereologi, Klimatologi dan Geofisika. Available online: https://www.bmkg.go.id/cuaca/prakiraan-cuaca.bmkg?Kec=Teunom&kab=Kab._Aceh_Jaya&Prov=Aceh&AreaID=5012629 (accessed on 10 March 2022).
57. Badan Pusat Staistik. *Aceh Jaya dalam Angka*; Badan Pusat Staistik: Calang, Indonesia, 2021.
58. USGS. Available online: <https://www.usgs.gov/> (accessed on 20 April 2022).
59. Badan Informasi Geospasial. Available online: <https://www.big.go.id/> (accessed on 20 April 2022).
60. BIG DEMNAS. Available online: <https://tanahair.indonesia.go.id/demnas/#/> (accessed on 28 June 2022).
61. Barber, A.J. The origin of the Woyla Terranes in Sumatra and the late Mesozoic evolution of the Sundaland margin. *J. Asian Earth Sci.* **2000**, *18*, 713–738. [[CrossRef](#)]
62. Saxon, E.; Sheppard, S. Land Systems of Indonesia and New Guinea. Available online: <https://databasin.org/datasets/eb74fe29b6fb49d0a6831498b0121c99/> (accessed on 27 July 2022).

63. Boeno, D.; Gubiani, P.I.; Lier, Q.; Van, J.; Mulazzani, R.P. Estimating lateral flow in double ring infiltrometer measurements. *Rev. Bras. Ciência Do Solo* **2021**, *45*, e0210027. [[CrossRef](#)]
64. Horton, R.E. An Approach Toward a Physical Interpretation of Infiltration-Capacity. *Soil Sci. Soc. Am. J.* **1941**, *5*, 399–417. [[CrossRef](#)]
65. de Oliveira, C.P.; de Lima, R.B.; Alves Junior, F.T.; de Lima Pessoa, M.M.; da Silva, A.F.; dos Santos, N.A.T.; Lopes, I.J.C.; de Melo, C.L.S.-M.S.; Silva, E.A.; da Silva, J.A.A.; et al. Dynamic Modeling of Land Use and Coverage Changes in the Dryland Pernambuco, Brazil. *Land* **2022**, *11*, 998.
66. Ahmad, F.; Goparaju, L.; Qayum, A. LULC analysis of urban spaces using Markov chain predictive model at Ranchi in India. *Spat. Inf. Res.* **2017**, *25*, 351–359. [[CrossRef](#)]
67. Marques, A.; Martins, I.S.; Kastner, T.; Plutzer, C.; Theurl, M.C.; Eisenmenger, N.; Huijbregts, M.A.J.; Wood, R.; Stadler, K.; Bruckner, M.; et al. Increasing impacts of land use on biodiversity and carbon sequestration driven by population and economic growth. *Nat. Ecol. Evol.* **2019**, *3*, 628–637. [[CrossRef](#)]
68. Li, Y.; Wu, W.; Liu, Y. Land consolidation for rural sustainability in China: Practical reflections and policy implications. *Land Use Policy* **2018**, *74*, 137–141. [[CrossRef](#)]
69. Ashaolu, E.D.; Olorunfemi, J.F.; Ifabiyi, I.P. Assessing the Spatio-Temporal Pattern of Land Use and Land Cover Changes in Osun Drainage Basin, Nigeria. *J. Environ. Geogr.* **2019**, *12*, 41–50. [[CrossRef](#)]
70. Msofe, N.K.; Sheng, L.; Lyimo, J. Land use change trends and their driving forces in the Kilombero Valley Floodplain, Southeastern Tanzania. *Sustainability* **2019**, *11*, 505. [[CrossRef](#)]
71. Veraart, A.J.; Dimitrov, M.R.; Schrier-Uijl, A.P.; Smidt, H.; de Klein, J.J.M. Abundance, Activity and Community Structure of Denitrifiers in Drainage Ditches in Relation to Sediment Characteristics, Vegetation and Land-Use. *Ecosystems* **2017**, *20*, 928–943. [[CrossRef](#)]
72. de Almeida, W.S.; Panachuki, E.; de Oliveira, P.T.S.; da Silva Menezes, R.; Sobrinho, T.A.; de Carvalho, D.F. Effect of soil tillage and vegetal cover on soil water infiltration. *Soil Tillage Res.* **2018**, *175*, 130–138. [[CrossRef](#)]
73. Portelinha, F.H.M.; Zornberg, J.G. Effect of infiltration on the performance of an unsaturated geotextile-reinforced soil wall. *Geotext. Geomembr.* **2017**, *45*, 211–226. [[CrossRef](#)]
74. Dawson, S.K.; Kingsford, R.T.; Berney, P.; Keith, D.A.; Hemmings, F.A.; Warton, D.I.; Waters, C.; Catford, J.A. Frequent inundation helps counteract land use impacts on wetland propagule banks. *Appl. Veg. Sci.* **2017**, *20*, 459–467. [[CrossRef](#)]
75. Seidl, M.; Hadrich, B.; Palmier, L.; Petrucci, G.; Nascimento, N. Impact of urbanisation (trends) on runoff behaviour of Pampulha watersheds (Brazil). *Environ. Sci. Pollut. Res.* **2020**, *27*, 14259–14270. [[CrossRef](#)]
76. Shrestha, S.; Cui, S.; Xu, L.; Wang, L.; Manandhar, B.; Ding, S. Impact of Land Use Change Due to Urbanisation on Surface Runoff Using GIS-Based SCS-CN Method: A Case Study of Xiamen City, China. *Land* **2021**, *10*, 839. [[CrossRef](#)]
77. Mu, B.; Zhao, X.; Zhao, J.; Liu, N.; Si, L.; Wang, Q.; Sun, N.; Sun, M.; Guo, Y.; Zhao, S. Quantitatively Assessing the Impact of Driving Factors on Vegetation Cover Change in China's 32 Major Cities. *Remote Sens.* **2022**, *14*, 839. [[CrossRef](#)]
78. Wu, H.; Cheng, S.; Li, Z.; Ke, G.; Liu, H. Study on Soil Water Infiltration Process and Model Applicability of Check Dams. *Water* **2022**, *11*, 1814. [[CrossRef](#)]
79. Scarpio, V.; Crema, S.; Marra, F.; Righini, M.; Ciccacese, G.; Borga, M.; Cavalli, M.; Corsini, A.; Marchi, L.; Surian, N.; et al. Basin-scale analysis of the geomorphic effectiveness of flash floods: A study in the northern Apennines (Italy). *Sci. Total Environ.* **2018**, *640–641*, 337–351. [[CrossRef](#)]
80. Zhang, X.; Lin, P.; Chen, H.; Yan, R.; Zhang, J.; Yu, Y.; Liu, E.; Yang, Y.; Zhao, W.; Lv, D.; et al. Understanding land use and cover change impacts on run-off and sediment load at flood events on the Loess Plateau, China. *Hydrol. Process.* **2018**, *32*, 576–589. [[CrossRef](#)]
81. Yang, J.Q.; Nepf, H.M. Impact of Vegetation on Bed Load Transport Rate and Bedform Characteristics. *Water Resour. Res.* **2019**, *55*, 6109–6124. [[CrossRef](#)]
82. Tang, X.; Hong, H.; Shu, Y.; Tang, H.; Li, J.; Liu, W. Urban waterlogging susceptibility assessment based on a PSO-SVM method using a novel repeatedly random sampling idea to select negative samples. *J. Hydrol.* **2019**, *576*, 583–595. [[CrossRef](#)]
83. Zhang, G.; Feng, G.; Li, X.; Xie, C.; Pi, X. Flood Effect on Groundwater Recharge on a Typical Silt Loam Soil. *Water* **2017**, *9*, 523. [[CrossRef](#)]